

Correlation-enhanced stability of microscopic cyclic heat engines

Guo-Hua Xu^{1,*} and Gentaro Watanabe^{1,2,†}

¹*Department of Physics and Zhejiang Institute of Modern Physics,
Zhejiang University, Hangzhou, Zhejiang 310027, China*

²*Zhejiang Province Key Laboratory of Quantum Technology and Device,
Zhejiang University, Hangzhou, Zhejiang 310027, China*

(Dated: August 5, 2022)

For cyclic heat engines operating in a finite cycle period, thermodynamic quantities have intercycle and intracycle correlations. By tuning the driving protocol appropriately, we can get the negative intercycle correlation to reduce the fluctuation of work through multiple cycles, which leads to the enhanced stability compared to the single-cycle operation. Taking the Otto engine with an overdamped Brownian particle as a working substance, we identify a scenario to get such enhanced stability by the intercycle correlation. Furthermore, we demonstrate that the enhancement can be readily realized in the current experiments for a wide range of protocols. By tuning the parameters within the experimentally achievable range, the uncertainty of work can be reduced to below $\sim 50\%$.

Introduction. With the advanced technology, various microscopic thermal devices have been fabricated on the submicron scale [1–10]. Among them, an important breakthrough for the exploration beyond conventional macroscopic thermodynamics is the experimental realization of the so-called Brownian heat engine [4–7], which consists of a Brownian particle subject to a time-dependent optical trap. In contrast to conventional macroscopic heat engines, fluctuations of thermodynamic quantities are significant in microscopic heat engines due to the small number of degrees of freedom in their working substance [11, 12]. In the past three decades, stochastic thermodynamics has been developed to formulate laws of thermodynamics for fluctuating thermodynamic quantities of small systems, and has had great success in understanding of thermodynamics of small systems [13–16]. Motivated by the experimental realization of microscopic heat engines and the theoretical advances in thermodynamics of small systems, there is a surge of activity on the study of microscopic heat engines [17–32]. Recently, fluctuations of the performance of microscopic heat engines and characterization of their performance beyond the mean values of thermodynamic quantities have become an active research topic [33–49].

Nevertheless, many studies of cyclic heat engines so far consider single-cycle operation and focus on the performance within a single cycle. In these studies, fluctuations of the thermodynamic quantities usually include only the intracycle correlation. In the quasistatic limit, since the thermal noise erases the correlation among thermodynamic quantities in different cycles [13, 38], it is sufficient to describe the fluctuations focusing on a single cycle. However, to get the nonzero power output, we need to operate engines in a finite cycle period. In this case, the effect of the intercycle correlation becomes non-negligible. Therefore, for engine operations over multiple cycles, assessing the performance within a single cycle is insufficient. Instead, assessments of the engine performance should address the global process over multiple cycles to include intercycle correlations.

Recently, fluctuations including intercycle correlations also started to be discussed. For example, various properties of the stochastic efficiency have been derived [50–56], and thermodynamic uncertainty relations which give a lower bound of uncertainties of the current [57–64] have been generalized for cyclic heat engines in the long-time limit [62–64].

However, the role of the time correlation in fluctuations of thermodynamic quantities has not been thoroughly explored. Since engines are supposed to operate over multiple cycles consecutively with a finite cycle period in practical situations, there is a great demand for a scheme to prevent the degradation of performance in multiple cycles by the intercycle correlation effect. In this Letter, by clarifying the effect of time correlation of work in microscopic heat engines with a finite cycle period, we identify such a scheme to reduce the fluctuation of work output. Since the fluctuation of work output is comparable to or even bigger than the average of work output in current experiments of small heat engines [4, 5], reducing the fluctuation of work output is a crucial issue. Taking an example of the Otto engine using a Brownian particle as a working substance, we demonstrate that the reduction of the fluctuation of work output can be realized in a robust manner in the current experiments, and this reduction can be more than 50%.

Setup. We study a small cyclic heat engine whose working substance is in contact with a heat bath with the controllable temperature $T(t)$ (we set the Boltzmann constant $k_B = 1$ throughout the Letter). The working substance is described by the Hamiltonian $H(\Gamma, t)$ with an external control parameter $\lambda(t)$, where Γ is the microstate of the working substance in the phase space. The engine is driven by time-periodically modulating T and λ with period τ , i.e., $T(t) = T(t + \tau)$ and $\lambda(t) = \lambda(t + \tau)$. Under such a protocol, we assume the engine is already driven into a periodic state with the probability distribution function (PDF) satisfying $p(\Gamma, t) = p(\Gamma, t + \tau)$ after running many cycles [20]. Therefore, we can represent time t by the phase as $\theta = 2\pi t/\tau$, and assign the initial phase θ_0 for the starting point of the cycle.

The work $W_{\theta_0}^{(n)}$ extracted through n cycles with the initial

* guohuax@zju.edu.cn

† gentaro@zju.edu.cn

phase θ_0 is a random variable given by

$$W_{\theta_0}^{(n)} = - \int_{\theta_0\tau/2\pi}^{n\tau+\theta_0\tau/2\pi} \frac{\partial H(\Gamma, t)}{\partial \lambda(t)} \dot{\lambda}(t) dt, \quad (1)$$

where the integral follows the Stratonovich rule [13]. The ensemble average $\langle W_{\theta_0}^{(n)} \rangle$ of work is independent of θ_0 , and satisfies $\langle W_{\theta_0}^{(n)} \rangle = n \langle W_{\theta_0}^{(1)} \rangle$, where $\langle \dots \rangle = \int \mathcal{D}[\Gamma(t)] p[\Gamma(t)] \dots$ is the path integral over all the possible trajectories $\Gamma(t)$.

The variance of work with initial time $t_0 = \theta_0\tau/(2\pi)$ is given by

$$\text{Var}[W_{\theta_0}^{(n)}] = \int_{t_0}^{n\tau+t_0} dt \int_{t_0}^{n\tau+t_0} dt' C(t, t'), \quad (2)$$

where the covariance function of power $\dot{W} \equiv -\partial_\lambda H(\Gamma, t) \dot{\lambda}(t)$ is defined as $C(t, t') \equiv \langle \dot{W}(t) \dot{W}(t') \rangle - \langle \dot{W}(t) \rangle \langle \dot{W}(t') \rangle$. The variance $\text{Var}[W_{\theta_0}^{(n)}]$ of work can be given by the sum of the contribution from each cycle, $n \text{Var}[W_{\theta_0}^{(1)}]$, and the remaining contribution denoted by $\mathcal{C}_{\theta_0}^{(n)}$:

$$\text{Var}[W_{\theta_0}^{(n)}] = n \text{Var}[W_{\theta_0}^{(1)}] + \mathcal{C}_{\theta_0}^{(n)}. \quad (3)$$

Here, the first term can be identified as the intracycle correlation within each single cycle and the second term $\mathcal{C}_{\theta_0}^{(n)}$ can be regarded as the intercycle correlation between different cycles. Since the system is not in a steady state, $\text{Var}[W_{\theta_0}^{(n)}]$ changes with θ_0 . However, the θ_0 -dependence is negligible for $n \rightarrow \infty$ because the correlation decays exponentially in time.

In this Letter, we use the single-cycle uncertainty $\Delta_{\theta_0}^{(1)} \equiv \text{Var}[W_{\theta_0}^{(1)}]/\langle W_{\theta_0}^{(1)} \rangle^2$ to describe the fluctuation of work within each single cycle. According to the law of large number, the uncertainty of work extracted through a large numbers n of cycles vanishes as $\sim 1/n$. Therefore, we use the scaled uncertainty Δ^∞ for infinite cycles defined as

$$\Delta^\infty = \lim_{n \rightarrow \infty} \Delta_{\theta_0}^{(n)} \equiv \lim_{n \rightarrow \infty} n \frac{\text{Var}[W_{\theta_0}^{(n)}]}{\langle W_{\theta_0}^{(n)} \rangle^2}. \quad (4)$$

Note that the θ_0 dependence of $\Delta_{\theta_0}^{(n)}$ vanishes in the limit of $n \rightarrow \infty$ because $\text{Var}[W_{\theta_0}^{(n)}]$ does so and $\langle W_{\theta_0}^{(n)} \rangle$ is independent of θ_0 . The multicycle uncertainty $\Delta_{\theta_0}^{(n)}$ ($n \geq 2$) defined in Eq. (4) is the quantity to be compared with $\Delta_{\theta_0}^{(1)}$. For a large cycle period, where the intercycle correlation is negligible, $\mathcal{C}_{\theta_0}^{(n)} \simeq 0$, $W_{\theta_0}^{(n)}$ is diffusive with $\text{Var}[W_{\theta_0}^{(n)}] = n \text{Var}[W_{\theta_0}^{(1)}]$, and we get $\Delta^\infty = \Delta_{\theta_0}^{(1)}$. On the other hand, for a small cycle period comparable to the relaxation time of the working substance, the intercycle correlation is significant. Our goal is to find an appropriate protocol which yields $\Delta^\infty < \Delta_{\theta_0}^{(1)}$ (i.e., $\mathcal{C}_{\theta_0}^\infty < 0$) for arbitrary θ_0 .

Relation between the single-cycle and multicycle uncertainties. To discuss the relationship between the uncertainties within a single cycle $\Delta_{\theta_0}^{(1)}$ and infinite cycles Δ^∞ , we consider an overdamped Brownian particle trapped in a one-dimensional harmonic oscillator potential with the Hamiltonian

$$H(x, t) = \frac{1}{2} \lambda(t) x(t)^2. \quad (5)$$

Here, $\lambda(t)$ is the stiffness of the potential which serves as a mechanical control parameter and $x(t)$ is the position of the Brownian particle. This system is described by the Ornstein-Uhlenbeck process [65]. The correlation function $\phi(t, t') \equiv \langle x(t)x(t') \rangle$ with $\phi(t, t') = \phi(t', t)$ is derived from the solution of the Itô stochastic differential equation for this process [66]. The resulting correlation function $\phi(t, t')$ for $t < t'$ is given by

$$\phi(t, t') = \phi(t, t) \exp \left[-\mu \int_t^{t'} ds \lambda(s) \right], \quad (6)$$

where μ is the mobility. In addition, since $\phi(t, t)$ is periodic in time, we have

$$\phi(t + \tau, t' + \tau) = \phi(t, t'). \quad (7)$$

The covariance function of power becomes $C(t, t') = \frac{1}{2} \dot{\lambda}(t) \dot{\lambda}(t') \phi(t, t')^2$ [66]. From Eqs. (6) and (7), we get the following properties of the covariance function: $C(t + \tau, t' + \tau) = C(t, t')$ and $C(t, t' + \tau) = aC(t, t')$, where $a \equiv \exp[-2\mu \int_0^\tau dt \lambda(t)] < 1$. Therefore, $C(t, t')$ decays exponentially in time when $|t - t'| \gg \tau$, and the correlation time of work is given by $\tau_{\text{corr}} = 2\mu \int_0^\tau dt \lambda(t)/\tau$.

From the above properties of $C(t, t')$, we can write the intercycle correlation $\mathcal{C}_{\theta_0}^{(2)}$ within the two successive cycles as $\mathcal{C}_{\theta_0}^{(2)} = [a + \gamma(\theta_0)] \text{Var}[W_{\theta_0}^{(1)}]$, where

$$\gamma(\theta_0) \equiv 2 \int_{\tau+t_0}^{2\tau+t_0} dt' \int_{t'-\tau}^{\tau+t_0} dt \frac{C(t, t')}{\text{Var}[W_{\theta_0}^{(1)}]}. \quad (8)$$

In the same way, we can write $\mathcal{C}_{\theta_0}^{(n)}$ in terms of a , $\gamma(\theta_0)$, and $\text{Var}[W_{\theta_0}^{(1)}]$ [66]. Then, the uncertainty for n cycles reads [66]

$$n \Delta_{\theta_0}^{(n)} = \left[(n - s_n) \frac{1 + \gamma(\theta_0)}{1 - a} + s_n \right] \Delta_{\theta_0}^{(1)}, \quad (9)$$

where $s_n \equiv (1 - a^n)/(1 - a) \geq 1$. For infinite cycles, we get

$$\frac{\Delta_{\theta_0}^{(1)}}{\Delta^\infty} = \frac{1 - a}{1 + \gamma(\theta_0)}. \quad (10)$$

For finite n cycles, the uncertainty derived from Eqs. (9) and (10) reads

$$\Delta_{\theta_0}^{(n)} = \left(1 - \frac{s_n}{n} \right) \Delta^\infty + \frac{s_n}{n} \Delta_{\theta_0}^{(1)}. \quad (11)$$

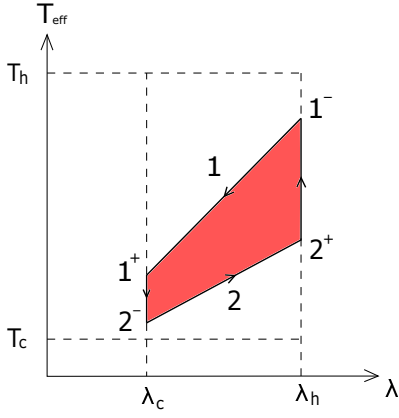


FIG. 1. Brownian Otto cycle with a finite cycle period on the λ - T_{eff} plane. Stroke 1 and 2 are isentropic expansion and compression, respectively. 1^+ (1^-) is the node after (before) the isentropic expansion and 2^+ (2^-) is the node after (before) the isentropic compression. Since the durations of isochoric strokes are finite, the effective temperature at nodes 1^- and 2^- are different from T_h and T_c , respectively.

If the intercycle correlation $\mathcal{C}_{\theta_0}^{(2)}$ is negative, i.e., $a + \gamma(\theta_0) < 0$, we get $\Delta_{\theta_0}^{(1)} > \Delta_{\theta_0}^{(n)} > \Delta^\infty$ from Eqs. (10) and (11) [67]. This means that the negative covariance of work between two successive cycles, $\mathcal{C}_{\theta_0}^{(2)} < 0$, indicates the reduction of uncertainty of work in multiple cycles. It is vice versa for the positive intercycle correlation. It is noted that the essential point of the above discussion is the exponential decay in time of the correlation functions. Even if the effect of inertia is non-negligible beyond the overdamped limit, the correlation functions can still be exponential in time with a smaller correlation time in the overdamped regime [66]. In addition, in the strongly underdamped regime, the correlation functions can be well approximated by an exponentially decaying function with a large correlation time $\tau_{\text{corr}} \simeq \gamma^{-1}$ obtained by averaging over the rapid oscillation [66]. Therefore, for the both cases, the above results can still apply, but with a different value of τ_{corr} .

It is possible to observe the enhanced stability due to the negative intercycle correlation when $\tau \lesssim \tau_{\text{corr}}$. To show this effect, below we consider a simple Brownian Otto engine, where the analytical result can be obtained. However, a similar result is also obtained for the Carnot cycle [66].

Results for the Brownian Otto cycle. Next, taking the Brownian Otto engine as an example, we demonstrate that the negative intercycle correlation can be realized in a wide range of parameters in the driving protocol. We still consider an overdamped Brownian particle in a harmonic oscillator potential described by the Ornstein-Uhlenbeck process. In this model, since the PDF $p(x, t)$ of any periodic state is Gaussian, we can define the effective temperature T_{eff} of the Brownian particle given by $T_{\text{eff}} = \lambda \langle x^2 \rangle$ [18]. The Brownian Otto engine consists of two isochoric and two isentropic strokes as shown in Fig. 1 [68]. During the hot (cold) isochoric strokes, the temperature T of the bath and the parameter λ are fixed at T_h and λ_h (T_c

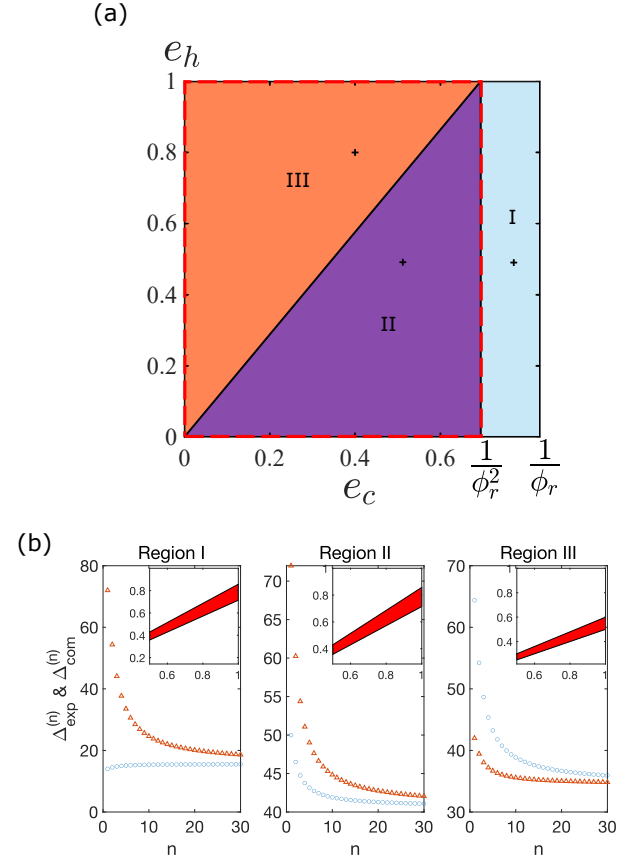


FIG. 2. Mapping out the regions of reduced fluctuation by the intercycle correlation. (a) The three regions with different order of the uncertainties: $\Delta_{\text{com}}^{(1)} > \Delta^\infty > \Delta_{\text{exp}}^{(1)}$ in region I, $\Delta_{\text{com}}^{(1)} > \Delta_{\text{exp}}^{(1)} > \Delta^\infty$ in region II, $\Delta_{\text{exp}}^{(1)} > \Delta_{\text{com}}^{(1)} > \Delta^\infty$ in region III. The uncertainties are reduced by the intercycle correlation in regions II and III, which are enclosed by the red dashed line. Here we set $\phi_r = 1.2$. (b) $\Delta_{\theta_0}^{(n)}$ as a function of n for a typical point [shown by the cross symbol in (a)] of each region. The blue circles show $\Delta_{\text{exp}}^{(n)}$ and the red triangles show $\Delta_{\text{com}}^{(n)}$. Insets of (b) show cycle diagrams on the λ - T_{eff} plane for each typical point. Here, we set $T_h = 1$, $\lambda_h = 1$, and $\lambda_c = 0.5$ for all the three cycle diagrams.

and λ_c), respectively, for the duration τ_h (τ_c) with $\lambda_c < \lambda_h$. During the isentropic strokes, T and λ are quenched simultaneously in a way such that the Shannon entropy $S \equiv -(\ln p)$ is unchanged [18]. We assume that the isentropic strokes are instantaneous, so that the cycle period is given by $\tau = \tau_h + \tau_c$.

For each m th cycle, we assign an odd integer $i = 2m - 1$ for the isentropic expansion stroke and an even integer $i = 2m$ for the isentropic compression stroke (see the strokes labeled “1” and “2” in Fig. 1 for $m = 1$). Since work is done only in the isentropic strokes, the fluctuation of work can take two values depending on whether θ_0 is in the hot or cold isochoric strokes. Therefore, the analysis can be divided into two cases according to the initial phase: the cycle starts before the isentropic expansion or compression. Then, we get the variance of work for the two cases, $\text{Var}[W_{\text{exp}}^{(1)}] = \sum_{i,j=1,2} C_{ij}$

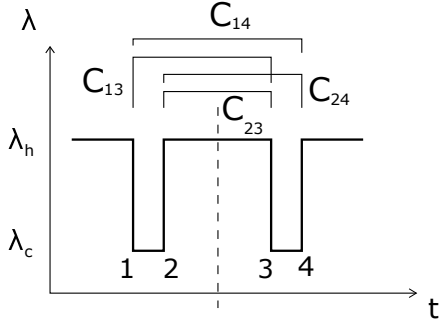


FIG. 3. Schematic diagram showing the contributions from the intercycle correlation for the Brownian Otto cycle starting before the isentropic expansion. Strokes 1 and 3 are isentropic expansion and strokes 2 and 4 are isentropic compression. The vertical dashed line represents the boundary between the cycles.

and $\text{Var}[W_{\text{com}}^{(1)}] = \sum_{i,j=2,3} C_{ij}$, respectively. Here, the subscript θ_0 in $W_{\theta_0}^{(1)}$ is replaced by “exp” and “com” for clarity, and $C_{ij} = \frac{1}{2}(\lambda_h - \lambda_c)^2 (-1)^{i-j} \phi_{ij}^2$. In this example, the correlation function $\phi_{ij} \equiv \phi(t_i, t_j)$ is analytically solvable [66].

From the analytical solution of ϕ_{ij} , one can find that the uncertainties $\Delta_{\text{exp}}^{(1)}$, $\Delta_{\text{com}}^{(1)}$, and Δ^∞ depend on three parameters [66]: $e_h \equiv \exp(-2\mu\lambda_h\tau_h)$, $e_c \equiv \exp(-2\mu\lambda_c\tau_c)$, and $\phi_r \equiv \phi_{11}/\phi_{22}$. Here, e_h and e_c are measures of the incompleteness of the equilibration in the hot and cold isochoric strokes, respectively, and ϕ_r describes the spread of the width of the PDF of the Brownian particle during the hot isochoric strokes. Since we are interested in the heat engine, the mean value of work should be positive, $\langle W^{(1)} \rangle = (\lambda_h - \lambda_c)(\phi_{11} - \phi_{22})/2 > 0$, and thus $\phi_r > 1$. In addition to the condition $\phi_r > 1$, the region of ϕ_r is upper bounded as $\phi_r < 1/e_c$ because the parameters e_h , e_c , and ϕ_r are constrained by [66]

$$\frac{(1 - e_h)(1 - \phi_r e_c)}{(1 - e_c)(\phi_r - e_h)} = R, \quad (12)$$

where $R \equiv T_c \lambda_h / (T_h \lambda_c)$ describes the reversibility with

$$\eta = 1 - \frac{\lambda_c}{\lambda_h} = 1 - \frac{1}{R} \frac{T_c}{T_h} < \eta_C. \quad (13)$$

Since $0 < e_c < 1$, $0 < e_h < 1 < \phi_r$, and $0 < R < 1$, we get $\phi_r < 1/e_c$ from Eq. (12).

Figure 2(a) is a region map showing which of the uncertainties $\Delta_{\text{exp}}^{(1)}$, $\Delta_{\text{com}}^{(1)}$, and Δ^∞ is smaller than the others. Regions II and III are of our interest, where the uncertainty Δ^∞ is smaller than those for a single cycle irrespective of the starting point of the cycle. Figure 2(a) tells that, if the equilibration in the cold isochoric strokes is sufficient with $e_c < 1/\phi_r^2$, we can get the reduction of the uncertainty for multiple cycles. It is noted that, to obtain this reduction, only the degree of equilibration in the cold isochoric strokes matters, but not that in the hot isochoric strokes.

We can provide a physical understanding of Fig. 2(a). An example of the protocol $\lambda(t)$ of the Brownian Otto engine starting before the isentropic expansion (stroke 1) is shown in

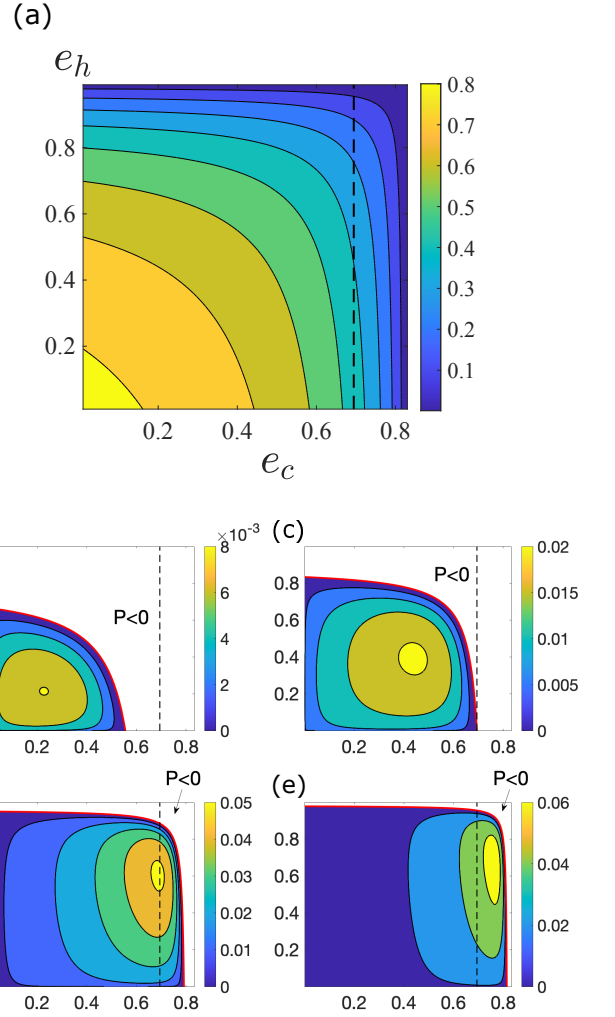


FIG. 4. (a) Product $R \equiv T_c \lambda_h / (T_h \lambda_c)$ of the compression ratio and the temperature ratio as a function of e_c and e_h . (b)-(e) Contour maps of the power as a function of e_c and e_h with given values of T_h/T_c , λ_h , and ϕ_r . Power is in units of $\mu \lambda_h T_h$. We set $T_h/T_c = 1.6$ [for (b)], 2.2 [for (c)], 5 [for (d)], and 10 [for (e)]. The red solid line shows $P = 0$. Since we only focus on the heat engine, values of P for the part with $P < 0$ are not shown here. In each figure, the vertical black dashed line shows $e_c = 1/\phi_r^2$. Here we set $\phi_r = 1.2$. The contour lines show the values next to the color bar.

Fig. 3. The intercycle correlation $\mathcal{C}_{\text{exp}}^{(2)} = C_{13} + C_{24} + C_{14} + C_{23}$ is represented by the four lines crossing the boundary between two cycles (vertical dashed line). From Eq. (6), the intercycle correlations in $\mathcal{C}_{\theta_0}^{(2)}$ satisfy $C_{i,i+1} = -e_c C_{ii}$ for odd i and $C_{i,i+1} = -e_h C_{ii}$ for even i . The correlation decays with n as $C_{i,j+2n} = a^n C_{ij}$, where $a = e_c e_h < 1$. Therefore, $\mathcal{C}_{\text{exp}}^{(2)}$ is proportional to $C_{11}a - C_{22}e_h \propto \phi_r^2 - 1/e_c$. As we have discussed, the necessary and sufficient condition for the reduction of uncertainty is $\mathcal{C}_{\theta_0}^{(2)} < 0$, which gives $e_c < 1/\phi_r^2$ corresponding to regions II and III. In the same way, for cycles starting before the isentropic compression, the intercycle correlation $\mathcal{C}_{\text{com}}^{(2)}$ is

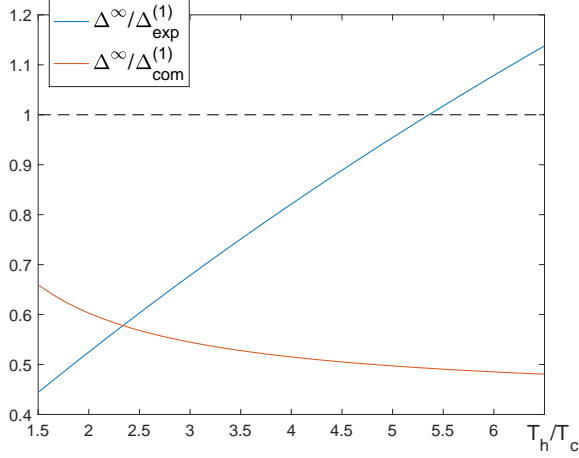


FIG. 5. $\Delta^\infty/\Delta_{\text{exp}}^{(1)}$ (blue line) and $\Delta^\infty/\Delta_{\text{com}}^{(1)}$ (red line) as functions of T_h/T_c with $T_c = 300$ K. Here we set $\mu = 0.119 \mu\text{m}\cdot\text{pN}^{-1}\cdot\text{ms}^{-1}$ [69, 70], $\lambda_c = 1.6 \text{ pN}\cdot\mu\text{m}^{-1}$, $\lambda_h = 2.4 \text{ pN}\cdot\mu\text{m}^{-1}$, $\tau_c = 0.7$ ms, and $\tau_h = 0.3$ ms. These parameters are achievable in the current experiment of Ref. [5]. The ratio $\Delta^\infty/\Delta_{\text{exp}}^{(1)}$ is still less than unity even at higher T_h beyond $T_h/T_c = 2$. In addition, the ratios $\Delta^\infty/\Delta_{\text{exp}}^{(1)}$ and $\Delta^\infty/\Delta_{\text{com}}^{(1)}$ can reach $\lesssim 50\%$.

given by $\mathcal{C}_{\text{com}}^{(2)} \propto 1 - \phi_r^2/e_h$, but it is always smaller than zero. Therefore, we have $\Delta^\infty < \Delta_{\text{com}}^{(1)}$ for arbitrary e_h . Summarizing the results for the above two cases, we get $\Delta^\infty < \Delta_{\text{exp}}^{(1)}$ and $\Delta_{\text{com}}^{(1)}$ provided $e_c < 1/\phi_r^2$. Namely, the fluctuation of work output is reduced in regions II and III for an arbitrary starting point. The difference between regions II and III is in the ordering of $\Delta_{\text{exp}}^{(1)}$ and $\Delta_{\text{com}}^{(1)}$ which depends on the intracycle correlation.

Finally, we discuss the role of the temperature of the bath and the experimental feasibility to get the reduction of the fluctuation by the intercycle correlation. First, we consider the mean value of the power P . As obtained in Ref. [71], P depends on six parameters: T_h , T_c , λ_h , λ_c , τ_h , and τ_c [66]. At any point in the region of $0 < e_c < 1$ and $0 < e_h < 1$, the power can be set to any positive value for a given ϕ_r by tuning the remaining free parameters, such as T_h , T_c , and λ_h . Figures 4(b)–4(e) show the power for different values of T_h/T_c . It can be seen that the point in the e_c - e_h plane giving the maximum power can be located in region I or II by tuning T_h/T_c . It is noted that we have $R > T_c/T_h$ for the Otto engine with $P > 0$ ($\eta > 0$) from Eq. (13). Second, we discuss the role of the temperature ratio T_h/T_c in the correlation-enhanced stability. Figure 4(a) shows a contour plot of R as a function of e_c and e_h for a fixed value of ϕ_r . As can be seen from Fig. 4(a), if R is larger than that at $e_c = 1/\phi_r^2$ and $e_h = 0$, it is guaranteed that we are in either region II or III. From Eq. (12), we find that this condition is $R > 1/(\phi_r + 1)$, or

$$\frac{T_c}{T_h} > \frac{\lambda_c/\lambda_h}{\phi_r + 1}. \quad (14)$$

A sufficient condition to satisfy this inequality is $T_h/T_c < 2$,

which is easy to realize in experiments. In experiments of microscopic heat engines with Brownian particles [4–6, 8, 9], one of the heat bath temperatures (commonly T_c) is usually set to be the room temperature: $T_c \sim 300$ K. In such a case, if T_h is $300 \text{ K} < T_h < 600 \text{ K}$ which is indeed the case in typical experiments [4, 5], it is guaranteed that the fluctuation of work in the Brownian Otto cycle is always reduced for multiple cycles irrespective of the other parameters. To demonstrate the large reduction of Δ^∞ by the intercycle correlation, we plot $\Delta^\infty/\Delta_{\text{exp}}^{(1)}$ and $\Delta^\infty/\Delta_{\text{com}}^{(1)}$ as functions of T_h/T_c in Fig. 5 for parameter values accessible in current experiments. Since the work output is zero at $T_h/T_c = \lambda_h/\lambda_c$ and increases with T_h/T_c , the region of T_h/T_c shown in Fig. 5 gives positive work output. It is noted that, compared to the above-mentioned sufficient condition, $T_h/T_c < 2$, for $\Delta^\infty < \Delta_{\text{exp}}^{(1)}$ and $\Delta_{\text{com}}^{(1)}$, we can obtain this reduction of Δ^∞ in a much wider temperature region of $T_h/T_c \lesssim 5.4$. Furthermore, the reduction of Δ^∞ over the single-cycle uncertainties can be very large by appropriately tuning the parameters and protocol. At $T_h/T_c \simeq 2.3$ where the red and blue lines cross, we have the same reduction rate for an arbitrary starting point. In this case, the uncertainty Δ^∞ can be reduced to less than 60% of the single-cycle uncertainties. If we set the starting point of the cycle before the isentropic compression stroke (i.e., the case of the red line), Δ^∞ can be reduced to even below 50% of the single-cycle uncertainty.

Conclusion. Our work has clarified the consequences of time correlation of work over different cycles in cyclic heat engines. If the cycle period is finite, focusing on one cycle is insufficient to discuss fluctuations of the performance of the microscopic heat engines. In particular, taking advantage of the intercycle correlation, the stability of the work output for the multicycle operation can be improved over the single-cycle one. Since such an improvement can be realized in a wide range of protocols, one can further optimize the other performance of the engine (such as efficiency, power, and uncertainty within each cycle). Furthermore, we have demonstrated that our findings can be readily realized in the current experiments. By tuning the parameters within the experimentally achievable range, the uncertainty of work output for infinite cycles can be reduced to less than 50% of the uncertainty for each single cycle. Since the fluctuation of work output can be even larger than the average of the work output in the current experiments [4, 5], our result should provide an important step toward the realization of microscopic heat engines for practical use. The effect of time correlation in other kinds of heat engines, such as autonomous heat engines and self-oscillating heat engines [24], is an interesting future problem.

ACKNOWLEDGMENTS

G. W. is supported by NSF of China (Grant No. 11975199), by the Zhejiang Provincial Natural Science Foundation Key Project (Grant No. LZ19A050001), and by the Zhejiang University 100 Plan.

- [1] T. Hugel, N. B. Holland, A. Cattani, L. Moroder, M. Seitz, and H. E. Gaub, Single-molecule optomechanical cycle, *Science* **296**, 1103 (2002).
- [2] P. G. Steeneken, K. Le Phan, M. J. Goossens, G. E. J. Koops, G. J. A. M. Brom, C. van der Avoort, and J. T. M. van Beek, Piezoresistive heat engine and refrigerator, *Nat. Phys.* **7**, 354 (2011).
- [3] S. Toyabe, T. Sagawa, M. Ueda, E. Muneyuki, and M. Sano, Experimental demonstration of information-to-energy conversion and validation of the generalized Jarzynski equality, *Nat. Phys.* **6**, 988 (2010).
- [4] V. Blickle and C. Bechinger, Realization of a micrometre-sized stochastic heat engine, *Nat. Phys.* **8**, 143 (2012).
- [5] I. A. Martínez, É. Roldán, L. Dinis, D. Petrov, J. M. R. Parrondo, and R. A. Rica, Brownian Carnot engine, *Nat. Phys.* **12**, 67 (2016).
- [6] A. Argun, J. Soni, L. Dabelow, S. Bo, G. Pesce, R. Eichhorn, and G. Volpe, Experimental realization of a minimal microscopic heat engine, *Phys. Rev. E* **96**, 052106 (2017).
- [7] S. Krishnamurthy, S. Ghosh, D. Chatterji, R. Ganapathy, and A. K. Sood, A micrometre-sized heat engine operating between bacterial reservoirs, *Nat. Phys.* **12**, 1134 (2016).
- [8] I. A. Martínez, É. Roldán, L. Dinis, and R. A. Rica, Colloidal heat engines: a review, *Soft Matter* **13**, 22 (2017).
- [9] S. Ciliberto, Experiments in Stochastic Thermodynamics: Short History and Perspectives, *Phys. Rev. X* **7**, 021051 (2017).
- [10] S. Erbas-Cakmak, D. A. Leigh, C. T. McTernan, and A. L. Nussbaumer, Artificial molecular machines, *Chem. Rev.* **115**, 10081 (2015).
- [11] C. Bustamante, J. Liphardt, and F. Ritort, The nonequilibrium thermodynamics of small systems, *Phys. Today* **58**, 43 (2005).
- [12] S. Ciliberto, S. Joubaud, and A. Petrosyan, Fluctuations in out-of-equilibrium systems: from theory to experiment, *J. Stat. Mech.* **2010**, P12003 (2010).
- [13] K. Sekimoto, *Stochastic Energetics* (Springer, Berlin, Heidelberg, 2010).
- [14] U. Seifert, Stochastic thermodynamics, fluctuation theorems and molecular machines, *Rep. Prog. Phys.* **75**, 126001 (2012).
- [15] U. Seifert, From Stochastic Thermodynamics to Thermodynamic Inference, *Annu. Rev. Condens. Matter Phys.* **10**, 171 (2019).
- [16] C. Jarzynski, Equalities and Inequalities: Irreversibility and the Second Law of Thermodynamics at the Nanoscale, *Annu. Rev. Condens. Matter Phys.* **2**, 329 (2011).
- [17] K. Sekimoto, F. Takagi, and T. Hondou, Carnot's cycle for small systems: Irreversibility and cost of operations, *Phys. Rev. E* **62**, 7759 (2000).
- [18] T. Schmiedl and U. Seifert, Efficiency at maximum power: An analytically solvable model for stochastic heat engines, *EPL* **81**, 20003 (2007).
- [19] V. Holubec, An exactly solvable model of a stochastic heat engine: optimization of power, power fluctuations and efficiency, *J. Stat. Mech.* **2014**, P05022 (2014).
- [20] K. Brandner, K. Saito, and U. Seifert, Thermodynamics of Micro- and Nano-Systems Driven by Periodic Temperature Variations, *Phys. Rev. X* **5**, 031019 (2015).
- [21] A. Dechant, N. Kiesel, and E. Lutz, All-optical nanomechanical heat engine, *Phys. Rev. Lett.* **114**, 183602 (2015).
- [22] A. Dechant, N. Kiesel, and E. Lutz, Underdamped stochastic heat engine at maximum efficiency, *EPL* **119**, 50003 (2017).
- [23] C. A. Plata, D. Guéry-Odelin, E. Trizac, and A. Prados, Building an irreversible Carnot-like heat engine with an overdamped harmonic oscillator, *J. Stat. Mech.* **2020**, 093207 (2020).
- [24] P. Strasberg, C. W. Wächter, and G. Schaller, Autonomous Implementation of Thermodynamic Cycles at the Nanoscale, *Phys. Rev. Lett.* **126**, 180605 (2021).
- [25] É. Fodor and M. E. Cates, Active engines: Thermodynamics moves forward, *EPL* **134**, 10003 (2021).
- [26] C. Van den Broeck, R. Kawai, and P. Meurs, Microscopic analysis of a thermal brownian motor, *Phys. Rev. Lett.* **93**, 090601 (2004).
- [27] R. Filliger and P. Reimann, Brownian gyrotor: A minimal heat engine on the nanoscale, *Phys. Rev. Lett.* **99**, 230602 (2007).
- [28] N. Shiraishi, K. Saito, and H. Tasaki, Universal trade-off relation between power and efficiency for heat engines, *Phys. Rev. Lett.* **117**, 190601 (2016).
- [29] O. Raz, Y. Subaşı, and R. Pugatch, Geometric heat engines featuring power that grows with efficiency, *Phys. Rev. Lett.* **116**, 160601 (2016).
- [30] M. Esposito, R. Kawai, K. Lindenberg, and C. Van den Broeck, Quantum-dot carnot engine at maximum power, *Phys. Rev. E* **81**, 041106 (2010).
- [31] O. Abah, J. Roßnagel, G. Jacob, S. Deffner, F. Schmidt-Kaler, K. Singer, and E. Lutz, Single-ion heat engine at maximum power, *Phys. Rev. Lett.* **109**, 203006 (2012).
- [32] V. Holubec and R. Marathe, Underdamped active brownian heat engine, *Phys. Rev. E* **102**, 060101(R) (2020).
- [33] N. A. Sinitsyn, Fluctuation relation for heat engines, *J. Phys. A: Math. Theor.* **44**, 405001 (2011).
- [34] S. Lahiri, S. Rana, and A. M. Jayannavar, Fluctuation relations for heat engines in time-periodic steady states, *J. Phys. A: Math. Theor.* **45**, 465001 (2012).
- [35] M. Campisi, Fluctuation relation for quantum heat engines and refrigerators, *J. Phys. A: Math. Theor.* **47**, 245001 (2014).
- [36] S. Rana, P. S. Pal, A. Saha, and A. M. Jayannavar, Single-particle stochastic heat engine, *Phys. Rev. E* **90**, 042146 (2014).
- [37] Y. Zheng and D. Poletti, Work and efficiency of quantum Otto cycles in power-law trapping potentials, *Phys. Rev. E* **90**, 012145 (2014).
- [38] K. Ito, C. Jiang, and G. Watanabe, Universal Bounds for Fluctuations in Small Heat Engines, (2019), [arXiv:1910.08096 \[cond-mat.stat-mech\]](https://arxiv.org/abs/1910.08096).
- [39] S. Saryal and B. K. Agarwalla, Bounds on fluctuations for finite-time quantum Otto cycle, *Phys. Rev. E* **103**, L060103 (2021).
- [40] S. Saryal, M. Gerry, I. Khait, D. Segal, and B. K. Agarwalla, Universal Bounds on Fluctuations in Continuous Thermal Machines, *Phys. Rev. Lett.* **127**, 190603 (2021).
- [41] K. Brandner and K. Saito, Thermodynamic Geometry of Microscopic Heat Engines, *Phys. Rev. Lett.* **124**, 040602 (2020).
- [42] H. J. D. Miller and M. Mehboudi, Geometry of Work Fluctuations versus Efficiency in Microscopic Thermal Machines, *Phys. Rev. Lett.* **125**, 260602 (2020).
- [43] G. Watanabe and Y. Minami, Finite-time thermodynamics of fluctuations in microscopic heat engines, *Phys. Rev. Research* **4**, L012008 (2022).
- [44] V. Holubec and A. Ryabov, Fluctuations in heat engines, *J. Phys. A: Math. Theor.* **55**, 013001 (2022).
- [45] Y. H. Chen, J.-F. Chen, Z. Fei, and H. T. Quan, A microscopic theory of curzon-ahlbom heat engine, (2021), [arXiv:2108.04128 \[cond-mat.stat-mech\]](https://arxiv.org/abs/2108.04128).
- [46] A. Dechant and S. -i. Sasa, Current fluctuations

- and transport efficiency for general langevin systems, *J. Stat. Mech.* **2018**, 063209 (2018).
- [47] A. C. Barato and R. Chetrite, Current fluctuations in periodically driven systems, *J. Stat. Mech.* **2018**, 053207 (2018).
- [48] C. Kwon, J. D. Noh, and H. Park, Work fluctuations in a time-dependent harmonic potential: Rigorous results beyond the overdamped limit, *Phys. Rev. E* **88**, 062102 (2013).
- [49] D. S. P. Salazar, Work distribution in thermal processes, *Phys. Rev. E* **101**, 030101(R) (2020).
- [50] G. Verley, M. Esposito, T. Willaert, and C. Van den Broeck, The unlikely Carnot efficiency, *Nat. Commun.* **5**, 4721 (2014).
- [51] G. Verley, T. Willaert, C. Van den Broeck, and M. Esposito, Universal theory of efficiency fluctuations, *Phys. Rev. E* **90**, 052145 (2014).
- [52] M. Poletini, G. Verley, and M. Esposito, Efficiency Statistics at All Times: Carnot Limit at Finite Power, *Phys. Rev. Lett.* **114**, 050601 (2015).
- [53] J.-H. Jiang, B. K. Agarwalla, and D. Segal, Efficiency Statistics and Bounds for Systems with Broken Time-Reversal Symmetry, *Phys. Rev. Lett.* **115**, 040601 (2015).
- [54] K. Proesmans, B. Cleuren, and C. Van den Broeck, Stochastic efficiency for effusion as a thermal engine, *EPL* **109**, 20004 (2015).
- [55] L. P. Fischer, P. Pietzonka, and U. Seifert, Large deviation function for a driven underdamped particle in a periodic potential, *Phys. Rev. E* **97**, 022143 (2018).
- [56] S. K. Manikandan, L. Dabelow, R. Eichhorn, and S. Krishnamurthy, Efficiency Fluctuations in Microscopic Machines, *Phys. Rev. Lett.* **122**, 140601 (2019).
- [57] A. C. Barato and U. Seifert, Thermodynamic Uncertainty Relation for Biomolecular Processes, *Phys. Rev. Lett.* **114**, 158101 (2015).
- [58] T. R. Gingrich, J. M. Horowitz, N. Perunov, and J. L. England, Dissipation Bounds All Steady-State Current Fluctuations, *Phys. Rev. Lett.* **116**, 120601 (2016).
- [59] J. Horowitz and T. Gingrich, Thermodynamic uncertainty relations constrain non-equilibrium fluctuations, *Nat. Phys.* **16**, 15 (2020).
- [60] P. Pietzonka and U. Seifert, Universal Trade-Off between Power, Efficiency, and Constancy in Steady-State Heat Engines, *Phys. Rev. Lett.* **120**, 190602 (2018).
- [61] V. Holubec and A. Ryabov, Cycling Tames Power Fluctuations near Optimum Efficiency, *Phys. Rev. Lett.* **121**, 120601 (2018).
- [62] A. C. Barato, R. Chetrite, A. Faggionato, and D. Gabrielli, Bounds on current fluctuations in periodically driven systems, *New J. Phys.* **20**, 103023 (2018).
- [63] T. Koyuk, U. Seifert, and P. Pietzonka, A generalization of the thermodynamic uncertainty relation to periodically driven systems, *J. Phys. A: Math. Theor.* **52**, 02LT02 (2018).
- [64] T. Koyuk and U. Seifert, Operationally Accessible Bounds on Fluctuations and Entropy Production in Periodically Driven Systems, *Phys. Rev. Lett.* **122**, 230601 (2019).
- [65] C. W. Gardiner, *Handbook of Stochastic Methods*, 3rd ed. (Springer, Berlin, 2004).
- [66] See Supplemental Material for details.
- [67] In this particular model, the sign of $\mathcal{C}_{\theta_0}^{(2)}$ and $\mathcal{C}_{\theta_0}^{\infty}$ are the same, so that the conditions $\mathcal{C}_{\theta_0}^{(2)} < 0$ and $\mathcal{C}_{\theta_0}^{\infty} < 0$ for $\Delta^{\infty} < \Delta_{\theta_0}^{(1)}$ are equivalent.
- [68] In experiments of the Brownian heat engines, adiabatic strokes are often replaced by isentropic strokes [5, 8, 72] since the working substance is always in contact with the environment (water), so that it is impossible to thermally isolate from the environment. In these isentropic strokes, the parameter λ and the temperature are controlled to keep the mean value of the entropy of the working substance constant.
- [69] P. Mestres, I. A. Martínez, A. Ortiz-Ambriz, R. A. Rica, and É. Roldán, Realization of nonequilibrium thermodynamic processes using external colored noise, *Phys. Rev. E* **90**, 032116 (2014).
- [70] From the viscosity η at room temperature $\eta = 0.89 \text{ pN}\cdot\mu\text{m}^{-2}$ and the radius of the Brownian particle $r = 0.5 \mu\text{m}$ given by Ref. [69], the mobility μ is obtained by $\mu = 1/(6\pi\eta r)$.
- [71] G.-H. Xu, C. Jiang, Y. Minami, and G. Watanabe, Relation between fluctuations and efficiency at maximum power for small heat engines (2022), [arXiv:2204.09939](https://arxiv.org/abs/2204.09939) [cond-mat.stat-mech].
- [72] I. A. Martínez, É. Roldán, L. Dinis, D. Petrov, and R. A. Rica, Adiabatic processes realized with a trapped brownian particle, *Phys. Rev. Lett.* **114**, 120601 (2015).

— Supplemental Material —
Correlation-enhanced Stability of Microscopic Cyclic Heat Engines

A. A. Derivation of the correlation function, Eq. (6)

Motion of a Brownian particle in a one-dimensional (1D) harmonic oscillator potential is a Gaussian process $x(t)$ described by the following Itô stochastic differential equation [S1]:

$$dx(t) = -\mu\lambda(t)x(t)dt + \sqrt{2\mu T(t)}dW(t), \quad (\text{S1})$$

where dW is the Wiener noise. The solution of Eq. (S1) is

$$x(t) = e^{-f(t)}x(0) + \int_0^t e^{-f(t)+f(s)}\sqrt{2\mu T(s)}dW(s) \quad (\text{S2})$$

with $f(t) \equiv \int_0^t \mu\lambda(s)ds$. Thus the mean value $\langle x(t) \rangle$ is given by

$$\langle x(t) \rangle = e^{-f(t)}\langle x(0) \rangle. \quad (\text{S3})$$

Because of the periodicity of the phase-space distribution function of the Brownian particle with the cycle period τ , we have $\langle x(\tau) \rangle = \langle x(0) \rangle$. Thus, together with Eq. (S3), we get $\langle x(\tau) \rangle = e^{-f(\tau)}\langle x(0) \rangle = \langle x(0) \rangle$, which leads to $\langle x(0) \rangle = 0$ since $f(\tau) \neq 0$. Therefore, the variance of $x(t)$ becomes $\text{Var}[x(t)] \equiv \langle (x(t) - \langle x(t) \rangle)^2 \rangle = \langle x^2(t) \rangle$.

The correlation function $\phi(t, t')$ is given by

$$\phi(t, t') \equiv \langle x(t)x(t') \rangle = e^{-[f(t)+f(t')]} \langle x^2(0) \rangle + \int_0^{\min(t, t')} e^{-[f(t)+f(t')-2f(s)]} 2\mu T(s) ds. \quad (\text{S4})$$

From the periodicity, $\langle x^2(\tau) \rangle = \langle x^2(0) \rangle$, and Eq. (S2), we have

$$\langle x^2(0) \rangle = \frac{2\mu \int_0^\tau e^{2f(t)} T(t) dt}{e^{2f(\tau)} - 1}. \quad (\text{S5})$$

Therefore, the correlation function $\phi(t, t')$ reads

$$\phi(t, t') = e^{-[f(t)+f(t')]} 2\mu \left[\int_0^{\min(t, t')} e^{2f(s)} T(s) ds + \frac{\int_0^\tau e^{2f(s)} T(s) ds}{e^{2f(\tau)} - 1} \right]. \quad (\text{S6})$$

For $t < t'$, $\phi(t, t')$ satisfies

$$\phi(t, t') = \phi(t, t) \exp \left[-\mu \int_t^{t'} ds \lambda(s) \right]. \quad (\text{S7})$$

1. The effect of inertia

As can be seen from Eq. (S7), the correlation function decays exponentially in the overdamped regime. Our results, Eqs. (10) and (11) of the main paper, are obtained from such exponentially decaying correlation function. Here, we show that, even if the inertia is non-negligible, the correlation functions can still be exponential in time in the strongly overdamped regime with $\gamma \gg \omega$, where $\omega = \sqrt{\lambda/m}$ is the frequency of the harmonic oscillator trapping potential and $m\gamma = \mu^{-1}$ is the frictional coefficient. In addition, in the strongly underdamped regime with $\gamma \ll \omega$, the correlation function can be well approximated by an exponentially decaying function in time obtained by averaging over the rapid oscillation. Therefore, for the both cases, the similar argument in the main paper can still apply with the effect of inertia, but τ_{corr} becomes smaller (larger) in the strongly overdamped (underdamped) regime compared to that in the overdamped limit. As a result, it is harder (easier) to observe the correlation-enhanced stability in the strongly overdamped (underdamped) regime because of the necessary condition: $\tau \lesssim \tau_{\text{corr}}$.

From the underdamped Langevin equation:

$$m\dot{v} = -m\gamma v - m\omega^2 x + \sqrt{2m\gamma T}\xi, \quad (\text{S8})$$

$$\dot{x} = v, \quad (\text{S9})$$

with $\xi = dW(t)/dt$, we can obtain the two-point correlation function of the positions of the Brownian particle [S2]:

$$\phi(0, t) = \langle x(t)x(0) \rangle = \frac{T}{m\omega^2} \frac{\Lambda_+ \exp(-\Lambda_- t) - \Lambda_- \exp(-\Lambda_+ t)}{\Lambda_+ - \Lambda_-} \quad (\text{S10})$$

with

$$\Lambda_{\pm} = \frac{\gamma}{2} \pm \sqrt{\left(\frac{\gamma}{2}\right)^2 - \omega^2}. \quad (\text{S11})$$

In the overdamped case with $\gamma \gg \omega$, we have $\Lambda_+ \gg \Lambda_-$ leading to

$$\phi(0, t) = \frac{T}{m\omega^2} \frac{\exp(-\Lambda_- t)}{1 - \frac{\Lambda_-}{\Lambda_+}}. \quad (\text{S12})$$

Therefore, the correlation function still shows exponential decay. Expand Λ_- to the second order of ω/γ , we have $\Lambda_- \simeq \mu\lambda[1 + (\omega/\gamma)^2] > \mu\lambda$, where $\lambda = m\omega^2$ and $\mu = (m\gamma)^{-1}$. It is noted that the correlation time, Λ_-^{-1} , is reduced from that in the overdamped limit, $(\mu\lambda)^{-1}$, due to the effect of inertia.

We assume that λ changes in a timescale $\lambda/\dot{\lambda}$ much larger than $2\pi/\omega$, and the correlation function oscillates with period $2\pi/\omega$ much smaller than τ in the strongly underdamped regime with $\gamma \ll \omega$ [S3]. Averaging over the coarse-grained timescale, which is sufficiently larger than $2\pi/\omega$ but sufficiently smaller than τ , the correlation function of work is given by

$$\overline{C(t, t')} = \frac{1}{2} \dot{\lambda}(t) \dot{\lambda}(t') \overline{\phi(t, t')^2}, \quad (\text{S13})$$

where “ $\overline{\quad}$ ” means the average over the coarse-grained timescale. In the timescale much smaller than $\lambda/\dot{\lambda}$, where the change of $\lambda \equiv m\omega^2$ is negligible, we have the following expression from Eq. (S10):

$$\begin{aligned} \phi(0, t)^2 &= \left(\frac{T}{m\omega^2} \frac{\Lambda_+ \exp(-\Lambda_- t) \Lambda_- \exp(-\Lambda_+ t)}{\Lambda_+ - \Lambda_-} \right)^2 \\ &= \left(\frac{T}{m\omega^2} \right)^2 \left(\frac{\gamma}{2\kappa} \sin \kappa t + \cos \kappa t \right)^2 \exp(-\gamma t) \end{aligned} \quad (\text{S14})$$

with

$$\kappa = \omega \sqrt{1 - \frac{1}{4} \left(\frac{\gamma}{\omega} \right)^2} = \omega + O[(\gamma/\omega)^2]. \quad (\text{S15})$$

Averaging over each oscillation period, we obtain

$$\overline{\phi(0, t)^2} \propto \exp(-\gamma t). \quad (\text{S16})$$

Therefore, also in the strongly underdamped regime of $\gamma \ll \omega$, the correlation function of work is well approximated by an exponentially decaying function in time with the large correlation time $\tau_{\text{corr}} = \gamma^{-1}$.

B. B. Derivation of Eq. (9)

Here, we give $\mathcal{E}_{\theta_0}^{(n)}$ in terms of a , $\gamma(\theta_0)$, and $\text{Var}[W_{\theta_0}^{(1)}]$. Recall that the variance $\text{Var}[W_{\theta_0}^{(n)}]$ of work is given by

$$\text{Var}[W_{\theta_0}^{(n)}] = \int_{t_0}^{n\tau+t_0} dt_1 \int_{t_0}^{n\tau+t_0} dt_2 C(t_1, t_2), \quad (\text{S17})$$

where the covariance function $C(t_1, t_2) \equiv 2^{-1} \dot{\lambda}(t_1) \dot{\lambda}(t_2) \phi(t_1, t_2)^2$ satisfies the following properties: $C(t_1 + \tau, t_2 + \tau) = C(t_1, t_2)$ and $C(t_1, t_2 + \tau) = aC(t_1, t_2)$ with $a \equiv \exp[-2\mu \int_0^\tau dt \dot{\lambda}(t)]$. The domain of the time-integration in the rhs of Eq. (S17) is shown

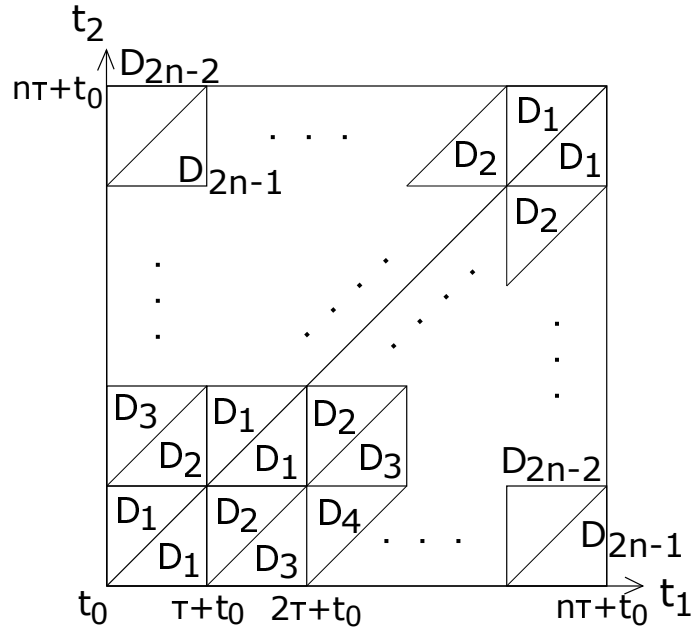


FIG. S1. Domain of the time-integration in the variance $\text{Var}[W_{\theta_0}^{(n)}]$ of work given by Eq. (S17). The horizontal (vertical) axis shows the integration variable t_1 (t_2) running from t_0 to $n\tau + t_0$. The whole domain of the integration is divided by $2n^2$ subdomains D_i with $i = 1, 2, \dots, 2n - 1$. Among these subdomains, equivalent ones are denoted by D_i with the same integer i .

in Fig. S1. In accordance with the periodicity of $C(t_1, t_2)$, $C(t_1 + \tau, t_2 + \tau) = C(t_1, t_2)$, equivalent subdomains are denoted by D_i with the same integer i . Now we introduce

$$d_i \equiv \int_{D_i} dt_1 dt_2 C(t_1, t_2), \quad (\text{S18})$$

and we have

$$d_1 = \text{Var}[W_{\theta_0}^{(1)}]/2, \quad (\text{S19})$$

$$d_2 = \text{Var}[W_{\theta_0}^{(1)}] \gamma(\theta_0)/2, \quad (\text{S20})$$

where

$$\gamma(\theta_0) \equiv 2 \int_{\tau+t_0}^{2\tau+t_0} dt_2 \int_{t_2-\tau}^{\tau+t_0} dt_1 \frac{C(t_1, t_2)}{\text{Var}[W_{\theta_0}^{(1)}]}, \quad (\text{S21})$$

and

$$d_{i+2} = a \cdot d_i \quad (\text{S22})$$

for $i \geq 2$.

For n cycles, the variance of work is given by

$$\begin{aligned} \text{Var}[W_{\theta_0}^{(n)}] &= 2 \sum_{k=0}^{n-1} (n-k) d_{2k+1} + 2 \sum_{k=1}^{n-1} (n-k) d_{2k} \\ &= \left[\left(n - s_n \right) \frac{1 + \gamma(\theta_0)}{1 - a} + s_n \right] \text{Var}[W_{\theta_0}^{(1)}]. \end{aligned} \quad (\text{S23})$$

Here, we have used the following summation formula of the series:

$$\sum_{k=0}^{n-1} (n-k) a^k = \frac{n - a \cdot s_n}{1 - a} \quad (\text{S24})$$

with $s_n \equiv (1 - a^n)/(1 - a)$. From Eq. (S23), the uncertainty for n cycles reads

$$n\Delta_{\theta_0}^{(n)} = \left[\left(n - s_n \right) \frac{1 + \gamma(\theta_0)}{1 - a} + s_n \right] \Delta_{\theta_0}^{(1)}. \quad (\text{S25})$$

From Eq. (S23), we can readily identify $\mathcal{E}_{\theta_0}^{(n)}$ as

$$\mathcal{E}_{\theta_0}^{(n)} = \frac{n - s_n}{1 - a} [a + \gamma(\theta_0)] \text{Var}[W_{\theta_0}^{(1)}]. \quad (\text{S26})$$

C. C: Covariance function of power for an overdamped Brownian particle trapped in a one-dimensional harmonic oscillator potential

For a Gaussian process, $x(t)$, all the higher-order correlation functions can be decomposed into products of two-point correlation functions using Wick's theorem [S7]. For example, we have

$$\langle x(t)^2 x(t')^2 \rangle = \langle x(t)^2 \rangle \langle x(t')^2 \rangle + 2 \langle x(t) x(t') \rangle^2. \quad (\text{S27})$$

Therefore, for an overdamped Brownian particle trapped in a one-dimensional harmonic oscillator potential with the Hamiltonian, $H(x, t) = \frac{1}{2} \lambda(t) x(t)^2$, the covariance function of power is given by

$$\begin{aligned} C(t, t') &= \langle \dot{W}(t) \dot{W}(t') \rangle - \langle \dot{W}(t) \rangle \langle \dot{W}(t') \rangle \\ &= \frac{1}{4} \dot{\lambda}(t) \dot{\lambda}(t') (\langle x(t)^2 x(t')^2 \rangle - \langle x(t)^2 \rangle \langle x(t')^2 \rangle) \\ &= \frac{1}{2} \dot{\lambda}(t) \dot{\lambda}(t') \phi(t, t')^2. \end{aligned} \quad (\text{S28})$$

D. D: Proof that $\Delta_{\text{exp}}^{(1)}$, $\Delta_{\text{com}}^{(1)}$, and Δ^∞ depend on three parameters: e_h , e_c , and ϕ_r

Here, we consider the Brownian Otto engine with the protocol defined in the main paper, and show that the uncertainties $\Delta_{\text{exp}}^{(1)}$, $\Delta_{\text{com}}^{(1)}$, and Δ^∞ depend on e_h , e_c , and ϕ_r . First, let us consider the case starting before an isentropic expansion stroke. The mean value $\langle W^{(1)} \rangle$ of work is given by

$$\langle W^{(1)} \rangle = \frac{1}{2} (\lambda_h - \lambda_c) (\phi_{11} - \phi_{22}) \quad (\text{S29})$$

with $\phi_{ij} \equiv \phi(t_i, t_j)$, where λ_h and λ_c are the stiffness of the potential during the hot and cold isochoric stroke, respectively. The variance $\text{Var}[W_{\text{exp}}^{(1)}]$ of work is given by

$$\text{Var}[W_{\text{exp}}^{(1)}] = \sum_{i,j=1,2} C_{ij} \quad (\text{S30})$$

with $C_{ij} \equiv C(t_i, t_j)$. Since $C_{ij} = 2^{-1} (\lambda_h - \lambda_c)^2 (-1)^{i-j} \phi_{ij}^2$ and $\phi_{12}^2 = e_c \phi_{11}^2$ with $e_c \equiv \exp(-2\mu \lambda_c \tau_c)$ and τ_c being the duration of the cold isochoric stroke, the uncertainty $\Delta_{\text{exp}}^{(1)} \equiv \text{Var}[W_{\text{exp}}^{(1)}] / \langle W^{(1)} \rangle^2$ is given by

$$\Delta_{\text{exp}}^{(1)} = 2 \frac{(1 - 2e_c) \phi_r^2 + 1}{(\phi_r - 1)^2} \quad (\text{S31})$$

with $\phi_r \equiv \phi_{11} / \phi_{22} > 1$. Similarly, in the case of starting before an isentropic compression stroke, the variance $\text{Var}[W_{\text{com}}^{(1)}]$ of work is given by

$$\text{Var}[W_{\text{com}}^{(1)}] = \sum_{i,j=2,3} C_{ij}. \quad (\text{S32})$$

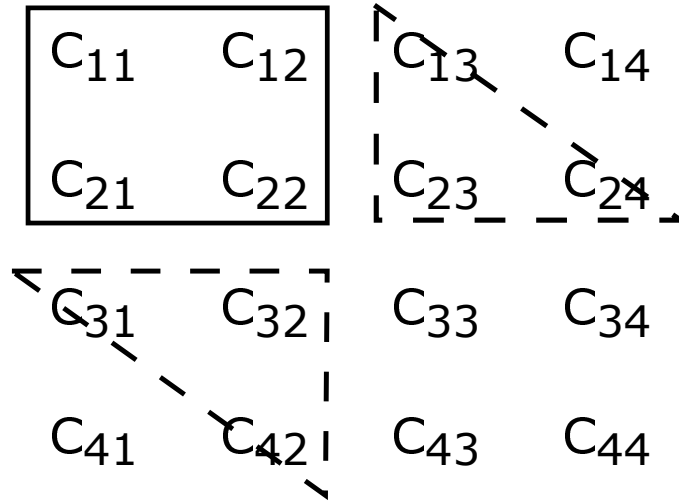


FIG. S2. Covariance matrix C_{ij} for two successive cycles starting before an isentropic expansion stroke. The sum of elements C_{ij} enclosed by the solid line equals $\text{Var}[W_{\text{exp}}^{(1)}]$, and the elements C_{ij} enclosed by the dashed lines contribute to γ_{exp} .

Since we have $\phi_{23}^2 = e_h \phi_{22}^2$ with $e_h \equiv \exp(-2\mu\lambda_h\tau_h)$ and τ_h being the duration of the hot isochoric stroke, the uncertainty $\Delta_{\text{com}}^{(1)}$ is given by

$$\Delta_{\text{com}}^{(1)} = 2 \frac{\phi_r^2 + (1 - 2e_h)}{(\phi_r - 1)^2}. \quad (\text{S33})$$

Finally, we discuss Δ^∞ . Since Δ^∞ is given by $\Delta^\infty = [1 + \gamma(\theta_0)](1 - a)^{-1} \Delta_{\theta_0}^{(1)}$, we focus on $\gamma(\theta_0)$, which is defined as Eq. (S21). For clarity, we write $\gamma(\theta_0)$ in the case of starting before an isentropic expansion (compression) stroke as γ_{exp} (γ_{com}). Here, we consider γ_{exp} as an example. Figure S2 shows the covariance matrix $C_{ij} \equiv C(t_i, t_j)$, which appears in the integrand of the expression of $\gamma(\theta_0)$ [Eq. (S21)]. For γ_{exp} , the elements of C_{ij} enclosed by the dashed lines contribute, so that γ_{exp} can be written as

$$\begin{aligned} \gamma_{\text{exp}} &= \frac{(C_{31} + C_{42}) + 2C_{32}}{\text{Var}[W_{\text{exp}}^{(1)}]} \\ &= a \frac{\phi_r^2 + (1 - 2e_c^{-1})}{(1 - 2e_c)\phi_r^2 + 1}. \end{aligned} \quad (\text{S34})$$

Similarly, γ_{com} can be written as

$$\gamma_{\text{com}} = a \frac{(1 - 2e_h^{-1})\phi_r^2 + 1}{\phi_r^2 + (1 - 2e_h)}. \quad (\text{S35})$$

Thus the uncertainty Δ^∞ for infinite cycles is given by

$$\Delta^\infty = \Delta_{\text{exp}}^{(1)} \frac{1 + \gamma_{\text{exp}}}{1 - a} = 2 \frac{(1 - 2e_c + e_c e_h)\phi_r^2 + (1 - 2e_h + e_c e_h)}{(1 - e_c e_h)(\phi_r - 1)^2}. \quad (\text{S36})$$

Therefore, from Eqs. (S31), (S33), and (S36), the uncertainties $\Delta_{\text{exp}}^{(1)}$, $\Delta_{\text{com}}^{(1)}$, and Δ^∞ depend on the three parameters: e_h , e_c , and ϕ_r . In addition, for n cycles, we obtain

$$\begin{aligned} \Delta_{\text{exp}}^{(n)} &= \left(1 - \frac{s_n}{n}\right) \Delta^\infty + \frac{s_n}{n} \Delta_{\text{exp}}^{(1)} \\ &= 2 \left(1 - \frac{1 - (e_c e_h)^n}{n(1 - e_c e_h)}\right) \frac{(1 - 2e_c + e_c e_h)\phi_r^2 + (1 - 2e_h + e_c e_h)}{(1 - e_c e_h)(\phi_r - 1)^2} + 2 \frac{1 - (e_c e_h)^n}{n(1 - e_c e_h)} \frac{(1 - 2e_c)\phi_r^2 + 1}{(\phi_r - 1)^2} \end{aligned} \quad (\text{S37})$$

and

$$\Delta_{\text{com}}^{(n)} = 2 \left(1 - \frac{1 - (e_c e_h)^n}{n(1 - e_c e_h)}\right) \frac{(1 - 2e_c + e_c e_h)\phi_r^2 + (1 - 2e_h + e_c e_h)}{(1 - e_c e_h)(\phi_r - 1)^2} + 2 \frac{1 - (e_c e_h)^n}{n(1 - e_c e_h)} \frac{\phi_r^2 + (1 - 2e_h)}{(\phi_r - 1)^2}. \quad (\text{S38})$$

E. E: Constraint on e_h , e_c , and ϕ_r : derivation of Eq. (12)

We consider the protocol starting from the adiabatic compression with $\lambda(t) = \lambda_h$ for $0 < t < \tau_h$, $\lambda(t) = \lambda_c$ for $\tau_h < t < \tau$, $T(t) = T_h$ for $0 < t < \tau_h$, and $T(t) = T_c$ for $\tau_h < t < \tau$, where $\lambda(t) = \lambda(t + \tau)$ and $T(t) = T(t + \tau)$. From Eq. (S6), the correlation function $\phi_{22} \equiv \phi(\tau, \tau) = \phi(0, 0)$ is given by

$$\begin{aligned}\phi_{22} &= 2\mu \frac{\int_0^\tau e^{2f(s)} T(s) ds}{e^{2f(\tau)} - 1} \\ &= \frac{1}{1 - e_c e_h} \left[\frac{T_c}{\lambda_c} (1 - e_c) + \frac{T_h}{\lambda_h} (1 - e_h) e_c \right].\end{aligned}\quad (\text{S39})$$

Here, we have used the following results: $\exp[2f(t)] = \exp(2\mu\lambda_h t)$ for $0 < t < \tau_h$, $\exp[2f(t)] = e_h^{-1} \exp[2\mu\lambda_c(t - \tau_h)]$ for $\tau_h < t < \tau$, $T(0^+) = T(\tau_h^-) = T_h$, and $T(\tau_h^+) = T(\tau^-) = T_c$. In the same way, the correlation function $\phi_{11} \equiv \phi(\tau_h, \tau_h)$ is given by

$$\begin{aligned}\phi_{11} &= e^{-[2f(\tau_h)]} 2\mu \left[\int_0^{\tau_h} e^{2f(s)} T(s) ds + \frac{\int_0^\tau e^{2f(s)} T(s) ds}{e^{2f(\tau)} - 1} \right] \\ &= 2\mu \frac{\int_{\tau_h}^{\tau+\tau_h} e^{2f(s)-2f(\tau_h)} T(s) ds}{e^{2f(\tau)} - 1} \\ &= \frac{1}{1 - e_c e_h} \left[\frac{T_c}{\lambda_c} (1 - e_c) e_h + \frac{T_h}{\lambda_h} (1 - e_h) \right].\end{aligned}\quad (\text{S40})$$

The ratio $\phi_r \equiv \phi_{11}/\phi_{22}$ reads

$$\phi_r = \frac{R(1 - e_c)e_h + (1 - e_h)}{R(1 - e_c) + (1 - e_h)e_c}, \quad (\text{S41})$$

which gives a constraint on e_h , e_c , and ϕ_r for the Otto engine:

$$\frac{(1 - e_h)(1 - \phi_r e_c)}{(1 - e_c)(\phi_r - e_h)} = R. \quad (\text{S42})$$

F. F: The role of e_h , e_c , and ϕ_r on the power

In the main paper, we have discussed about the correlation-enhanced stability in the Brownian Otto engine, and we have found that the uncertainty of work depends only on the three parameters: e_h , e_c , and ϕ_r . Here, we show that the mean value of power for given e_h , e_c , and ϕ_r can reach arbitrary value for $0 < e_c < 1$ and $0 < e_h < 1$. In addition, we give a detailed calculation of the power plotted in Figs. 4(b)–4(e).

Power of the Brownian Otto engine is given by [S5]

$$P = \frac{(1 - \lambda_c/\lambda_h) [(\lambda_c/\lambda_h) T_h - T_c]}{(\lambda_c/\lambda_h) (\tau_h + \tau_c)} \frac{\sinh(\mu\lambda_c\tau_c) \sinh(\mu\lambda_h\tau_h)}{\sinh(\mu\lambda_c\tau_c + \mu\lambda_h\tau_h)}, \quad (\text{S43})$$

which depends on six parameters: T_h , T_c , λ_h , λ_c , τ_h , and τ_c . At any point in Fig. 2(a), only three parameters are given: $e_h = \exp(-2\mu\lambda_h\tau_h)$, $e_c = \exp(-2\mu\lambda_c\tau_c)$, and ϕ_r . Here, ϕ_r can be substituted by $R = T_c\lambda_h/(T_h\lambda_c)$ from Eq. (12). Therefore, we can still choose arbitrary positive values for the remaining three of the six parameters. For example, when $\lambda_h\tau_h$, $\lambda_c\tau_c$, and R are given, we can still choose arbitrary positive values for T_h , T_c , and λ_h with $T_c/T_h < R$. Here, the constraint on T_c/T_h is from the fact that $\eta = 1 - \lambda_c/\lambda_h = 1 - (T_c/T_h)/R > 0$ for the Otto engine. In this case, we can rewrite Eq. (S43) as follows:

$$P = -\mu T_h \lambda_h \frac{R - T_c/T_h}{\ln e_h + (RT_h/T_c) \ln e_c} \frac{(1 - R)}{R} \frac{(1 - e_c)(1 - e_h)}{1 - e_c e_h}. \quad (\text{S44})$$

Since there is no bound on T_h or λ_h in our discussion, power can take any positive value. Figures 4(b)–4(e) show the power as a function of e_c and e_h for given values of T_h , T_c , λ_h , and ϕ_r obtained from Eq. (S44) and (S42).

G. G: Correlation-enhanced stability for the Carnot cycle

We discuss the effect of intercycle correlation in the Carnot cycle with the model by Schmiedl and Seifert [S6]. We calculate the uncertainty of work output at maximum power for the Carnot cycle, and show that the negative intercycle correlations can be obtained in some regions of the parameter space for the Carnot cycle as well.

In this model, the working substance is an overdamped Brownian particle trapped in a harmonic oscillator potential. According to Ref. [S6], the cycle consists of two adiabatic jumps and two isothermal strokes. The durations of the adiabatic strokes are negligible and those of the hot and cold isothermal strokes are τ_h and τ_c , respectively. During the hot (cold) isothermal stroke, $0 < t < \tau_h$ ($\tau_h < t < \tau = \tau_h + \tau_c$), the water temperature T_h (T_c) is constant. The heat engine protocol $\lambda(t)$ is optimized to yield the maximum work output with given boundary values of the variance of the particle position x : $\sigma_{\min} \equiv \sigma(0) = \sigma(\tau)$ and $\sigma_{\max} = \sigma(\tau_h)$, where $\sigma \equiv \langle x^2 \rangle - \langle x \rangle^2$. Since the power is nonzero at each moment, $\dot{W} \neq 0$, the correlation of work for the Carnot cycle is more complicated than that for the Otto cycle considered in the main paper. From our numerical result, we find that the uncertainty of work at maximum power depends only on the ratio $\sigma_r \equiv \sigma_{\min}/\sigma_{\max}$ and $\eta_C \equiv 1 - T_c/T_h$. Figure S3 shows that there are some regions (regions II and III) in the parameter space where we have the correlation-enhanced stability.

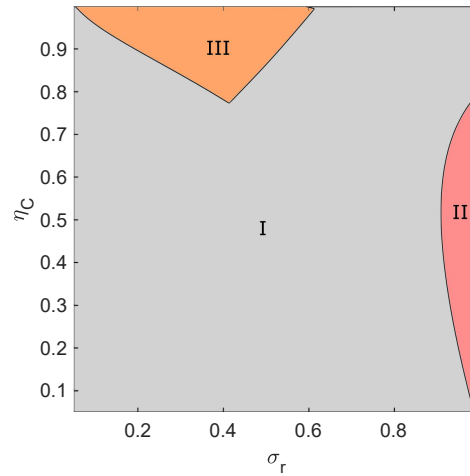


FIG. S3. Mapping out the regions of the correlation-enhanced stability for the Carnot cycle with the model by Schmiedl and Seifert [S6]. Δ^∞ is compared to $\Delta_{\theta_0}^{(1)}$ with the starting point $t_0 = 0^+$, τ_h^- , τ_h^+ , or τ^- corresponding to the node in the Carnot cycle. In regions II and III, Δ^∞ is smaller than $\Delta_{\theta_0}^{(1)}$ for any of the four choices of t_0 .

-
- [S1] C. W. Gardiner, *Handbook of Stochastic Methods*, 3rd ed. (Springer, Berlin, 2004).
 - [S2] A. G. Frim and M. R. DeWeese, Optimal finite-time Brownian Carnot engine, *Phys. Rev. E* **105**, L052103 (2022).
 - [S3] A. Dechant, N. Kiesel, and E. Lutz, Underdamped stochastic heat engine at maximum efficiency, *EPL* **119**, 50003 (2017).
 - [S4] I. A. Martínez, É. Roldán, L. Dinis, D. Petrov, J. M. R. Parrondo, and R. A. Rica, Brownian Carnot engine, *Nat. Phys.* **12**, 67 (2016).
 - [S5] G.-H. Xu, C. Jiang, Y. Minami, and G. Watanabe, Relation between fluctuations and efficiency at maximum power for small heat engines, arXiv:2204.09939 [cond-mat.stat-mech].
 - [S6] T. Schmiedl and U. Seifert, Efficiency at maximum power: An analytically solvable model for stochastic heat engines, *EPL* **81** 20003 (2008).
 - [S7] R. Kubo, M. Toda, and N. Hashitsume, *Statistical Physics 2*, 2nd ed. (Springer, 1991).